

## Deriving vegetation drag coefficients in combined wave-current flows by calibration and direct measurement methods

Chen, Hui; Ni, Yan; Li, Yulong; Liu, Feng; Ou, Suying; Su, Min; Peng, Yisheng; Hu, Zhan; Uijttewaal, Wim; Suzuki, Tomohiro

**DOI**

[10.1016/j.advwatres.2018.10.008](https://doi.org/10.1016/j.advwatres.2018.10.008)

**Publication date**

2018

**Document Version**

Final published version

**Published in**

Advances in Water Resources

**Citation (APA)**

Chen, H., Ni, Y., Li, Y., Liu, F., Ou, S., Su, M., Peng, Y., Hu, Z., Uijttewaal, W., & Suzuki, T. (2018). Deriving vegetation drag coefficients in combined wave-current flows by calibration and direct measurement methods. *Advances in Water Resources*, 122, 217-227. <https://doi.org/10.1016/j.advwatres.2018.10.008>

**Important note**

To cite this publication, please use the final published version (if applicable).  
Please check the document version above.

**Copyright**

Other than for strictly personal use, it is not permitted to download, forward or distribute the text or part of it, without the consent of the author(s) and/or copyright holder(s), unless the work is under an open content license such as Creative Commons.

**Takedown policy**

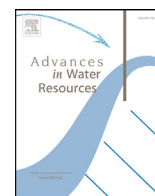
Please contact us and provide details if you believe this document breaches copyrights.  
We will remove access to the work immediately and investigate your claim.

***Green Open Access added to TU Delft Institutional Repository***

***'You share, we take care!' – Taverne project***

**<https://www.openaccess.nl/en/you-share-we-take-care>**

Otherwise as indicated in the copyright section: the publisher is the copyright holder of this work and the author uses the Dutch legislation to make this work public.



## Deriving vegetation drag coefficients in combined wave-current flows by calibration and direct measurement methods

Hui Chen<sup>a,b,c</sup>, Yan Ni<sup>d</sup>, Yulong Li<sup>a,b,c</sup>, Feng Liu<sup>a,b,c</sup>, Suying Ou<sup>a,b,c</sup>, Min Su<sup>a,b,c</sup>, Yisheng Peng<sup>e</sup>, Zhan Hu<sup>a,b,c,\*</sup>, Wim Uijttewaal<sup>f</sup>, Tomohiro Suzuki<sup>f,g</sup>

<sup>a</sup> Institute of Estuarine and Coastal Research, School of Marine Science, Sun Yat-sen University, Guangzhou 510275, China

<sup>b</sup> State-Province Joint Engineering Laboratory of Estuarine Hydraulic Technology, Guangzhou 510275, China

<sup>c</sup> Guangdong Province Engineering Research Center of Coasts, Islands and Reefs, Guangzhou 510275, China

<sup>d</sup> Shanghai Waterway Engineering Design and Consulting Co., Ltd., Shanghai 200120, China

<sup>e</sup> School of Environmental Science and Engineering/Research Center of Wetland Science, Sun Yat-Sen University, Guangzhou 501275, China

<sup>f</sup> Faculty of Civil Engineering and Geosciences, Delft University of Technology, Stevinweg 1, Delft 2628 CN, the Netherlands

<sup>g</sup> Flanders Hydraulics Research, Berchemlei 115, Antwerp 2140, Belgium

### ARTICLE INFO

#### Keywords:

Wave dissipation  
Vegetation  
Drag coefficient  
Wave-current interaction  
Keulegan-Carpenter number  
Flume experiment

### ABSTRACT

Coastal vegetation is efficient in damping incident waves even in storm events, thus providing valuable protections to coastal communities. However, large uncertainties lie in determining vegetation drag coefficients ( $C_D$ ), which are directly related to the wave damping capacity of a certain vegetated area. One major uncertainty is related to the different methods used in deriving  $C_D$ . Currently, two methods are available, i.e. the conventional calibration approach and the new direct measurement approach. Comparative studies of these two methods are lacking to reveal their respective strengths and reduce the uncertainty. Additional uncertainty stems from the dependence of  $C_D$  on flow conditions (i.e. wave-only or wave-current) and indicative parameters, i.e. Reynolds number ( $Re$ ) and Keulegan-Carpenter number ( $KC$ ). Recent studies have obtained  $C_D-Re$  relations for combined wave-current flows, whereas  $C_D-KC$  relations in such flow condition remain unexplored. Thus, this study conducts a thorough comparison between two existing methods and explores the  $C_D-KC$  relations in combined wave-current flows. By a unique revisiting procedure, we show that  $C_D$  derived by the direct measurement approach have a better overall performance in reproducing both acting force and the resulting wave dissipation. Therefore, a generic  $C_D-KC$  relation for both wave-only and wave-current flows is proposed using direct measurement approach. Finally, a detailed comparison of these two approaches are given. The comprehensive method comparison and the obtained new  $C_D-KC$  relation may lead to improved understanding and modelling of wave-vegetation interaction.

### 1. Introduction

Upright vegetation in coastal wetlands can significantly attenuate incident wave energy, thus providing protections to coastal habitats and structures (Anderson et al., 2011; Vuik et al., 2016, 2018). The wave damping effect is significant even in storm conditions (Möller et al., 2014). Additionally, natural vegetation ecosystems can adjust their bed elevation to sea level rise via ecogeomorphological feedbacks, which enables long-term sustainable coastal defense solutions (Arkema et al., 2013; D'Alpaos and Marani, 2016; D'Alpaos et al., 2016; Temmerman and Kirwan, 2015). With increasing storminess in the future (Donnelly et al., 2004; Young et al., 2011), the protection offered by coastal vegetation can be of greater importance.

Wave energy dissipation by vegetation (hereafter referred as  $WDV$ ) is affected by incident wave height ( $H$ , Méndez and Losada, 2004; Bradley and Houser, 2009), wave period ( $T$ , Augustin et al., 2009; Suzuki et al., 2012), the ratio of water depth to vegetation height in the water ( $h/h_v$ , Ysebaert et al., 2011; Yang et al., 2012), drag coefficient ( $C_D$ , Henry et al., 2015; Losada et al., 2016a,b), stiffness (Bouma et al., 2005; Luhar et al., 2017; Paul et al., 2016) and stem frontal area of plants per unit height (i.e.  $N^*b_v$ ,  $N$  is the number of stems per unit area and  $b_v$  is the stem diameter, Augustin et al., 2009; Fonseca and Cahalan, 1992; Nepf, 2012, 1999; Ozeren et al., 2014). This knowledge has also been adapted in different numerical models (e.g. Augustin et al., 2009; Cao et al., 2015; Maza et al., 2013; Suzuki et al., 2012). Recent experimental studies have also identified  $WDV$  is affected by co-existing currents (Li and Yan, 2007; Paul et al., 2012; Hu et al., 2014; Losada et al., 2016a,b).

\* Corresponding author at: Institute of Estuarine and Coastal Research, School of Marine Science, Sun Yat-sen University, No. 135, Xingang Xi Road, Guangzhou 510275, China.

E-mail address: [huzh9@mail.sysu.edu.cn](mailto:huzh9@mail.sysu.edu.cn) (Z. Hu).

<https://doi.org/10.1016/j.advwatres.2018.10.008>

Received 12 February 2018; Received in revised form 4 October 2018; Accepted 11 October 2018

Available online 16 October 2018

0309-1708/© 2018 Elsevier Ltd. All rights reserved.

**Table 1**  
A review of  $C_D$  relations in vegetation-wave interaction and their deriving methods.

Reference	Mimic Type	Flow condition	$C_D$ relation	Deriving method
Kobayashi et al. (1993)	Flexible plastic strips	Waves	$C_D = 0.08 + (2200/Re)^{2.4}$ $2200 < Re < 18,000$	Calibration method
Méndez et al. (1999)	Flexible plastic strips	Waves	$C_D = 0.08 + (2200/Re)^{2.2}$ $2000 < Re < 15,500$ (no swaying) $C_D = 0.40 + (4600/Re)^{2.9}$ $2300 < Re < 20,000$ (swaying)	Calibration method
Mendez and Losada (2004)	Flexible real vegetation	Waves	$C_D = 0.47 \exp(-0.052KC)$ $R^2 = 0.76$ $3 \leq KC \leq 59$	Calibration method
Bradley and Houser (2009)	Flexible real vegetation	Waves	$C_D = 253.9KC^{-3.0}$ $R^2 = 0.95$ $0 < KC < 6$ Field data Calculated using the relative velocity of the seagrass blades	Calibration method
Ranjit S. Jadhav et al. (2013)	Flexible real vegetation	Waves	$C_D = 70KC^{-0.86}$ $R^2 = 0.95$ $25 < KC < 135$	Calibration method
Anderson and Smith (2014)	Flexible plastic strips	Waves	$C_D = 1.10 + (27.4/KC)^{3.08}$ $R^2 = 0.88$ $26 < KC < 112$ $C_D = 0.76 + (744.2/Re)^{1.27}$ $R^2 = 0.94$ $533 < Re < 2296$	Calibration method
Ozeren et al. (2014) <sup>b</sup>	Rigid wooden cylinders	Waves	$C_D = 1.5 + (6.785/KC)^{2.22}$ $R^2 = 0.21$ $N_v = 156m^{-2}$ , $h_v = 0.63m$ $C_D = 2.1 + (793/Re)^{2.39}$ $C_D = 0.683 + (12.07/KC)^{2.25}$ $N_v = 350m^{-2}$ , $h_v = 0.48m$	Calibration method
Infantes et al. (2011)	Flexible real vegetation	Waves	$\lg C_D = -0.6653 \cdot \lg Re + 1.1886$ $R^2 = 0.77$	Direct measurement method
Hu et al. (2014)	Rigid wooden cylinders	Wave + Current	$C_D = 1.04 + (730/Re)^{1.37}$ $R^2 = 0.66$ $300 < Re < 4700$	Direct measurement method
Losada et al. (2016a,b)	Flexible real vegetation	Wave $\pm$ Current	$C_D = 0.08 + (50,000/Re)^{2.2}$ $R^2 = 0.60$ (regular waves) $C_D = 0.25 + (75,000/Re)^9$ (regular waves + currents) $C_D = 0.50 + (50,000/Re)^9$ (regular waves-currents)	Calibration method

WDV is mainly induced by the drag force provided by the vegetation acting on the water motion, which can be quantified by Morison equation (Dalrymple et al., 1984; Morison et al., 1950). The drag force ( $F_d$ ) is proportional to the square of the velocity, vegetation frontal area and vegetation drag coefficient ( $C_D$ ). Thus, choosing suitable  $C_D$  values is of vital importance to accurate WDV prediction. The parameterization of  $C_D$  is currently one of the major difficulties in modeling the interactions between vegetation and water motion (Suzuki et al., 2012; Luhar and Nepf, 2013; Maza et al., 2015a; Cao et al., 2015). Thus, determining  $C_D$  has been a main subject in numerous existing studies (see Table 1).

$C_D$  is typically determined by experiments, either by calibration or direct measurement approach (Table 1). The calibration approach is a conventional method, which determines  $C_D$  by calibrating its value in WDV models to fit the measured wave height reduction (e.g. Mendez et al., 1999; Augustin et al., 2009). Previously, this method could not be applied in the cases of vegetation in combined wave-current flows, as previous models did not take into account the influence of co-existing current on WDV (Dalrymple et al., 1984). This limitation has recently been relaxed by a new model proposed by Losada et al. (2016a,b), which can explicitly account for WDV in combined wave-current flows. Thus, the calibration method can now be applied to derive  $C_D$  in both wave-only and combined wave-current conditions. Compared to the calibration method, the direct measurement method is a new approach (Hu et al., 2014). This approach is based on the original Morison equation instead of WDV models, and it requires synchronized impact velocity and force data to derive  $C_D$  by quantifying the work done by the drag force over one wave period. As the Morison equation holds in both

wave-only and wave-current flows, this approach can be applied to derive  $C_D$  in both flow conditions. Thus, a vegetation drag coefficient  $C_D$  in wave-only and wave-current flows can be obtained by both calibration and direct measurement methods. However, the merits and drawbacks of these two methods have not been explored in parallel. A detailed comparison of these two methods can be valuable for future experimental and numerical studies.

Many previous studies have identified that vegetation drag coefficient  $C_D$  in oscillatory flows (i.e. wave-only or combined wave-current) varies with Reynolds number ( $Re$ ) (see Table 1 and Fig. 1a). The obtained  $C_D$ - $Re$  relations all show that  $C_D$  decreases with increasing  $Re$ . It is similar to those derived from unidirectional flows conditions, but  $C_D$  values have greater range of variation (0.1 to 100) in oscillatory flows (Nepf, 2012). Most of the previous  $C_D$ - $Re$  relations are obtained in either wave-only or current-only condition. It is only until recently that new  $C_D$ - $Re$  relations are extended to combined wave-current flow conditions (Hu et al., 2014; Losada et al., 2016a,b). Such an extension is of importance as the combined wave-current flows are common in e.g. natural wetlands. Besides  $C_D$ - $Re$  relations,  $C_D$  in oscillatory flows has been found to be a function of Keuglan-Carpenter ( $KC$ ) number (see Table 1 and Fig. 1b). Mendez and Losada, (2004) found that  $C_D$ - $KC$  relations are more suitable for oscillatory flows compared to  $C_D$ - $Re$  relations. However,  $C_D$ - $KC$  relations have only been explored in wave-only conditions so far (see Table 1 and Fig. 1b). Thus, such relations in combined current-wave flows are yet to be explored.

In this study, we aim to provide 1) a thorough comparison between the calibration and direct measurement methods, and 2) a generic  $C_D$ -

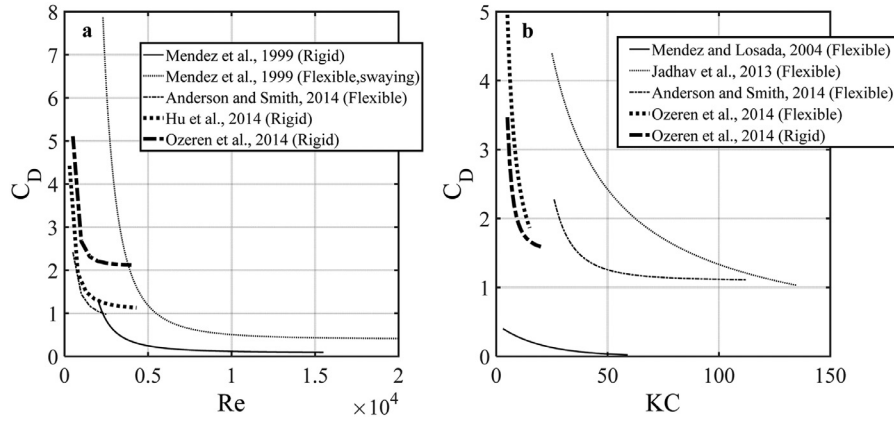


Fig. 1. Selected  $C_D$ -Re (panel a) and  $C_D$ -KC (panel b) relations from previous studies that listed in the Table 1.

KC relation for various oscillatory flows, i.e. wave-only and combined wave-current flows. To our knowledge, the current study is the first study to provide a detailed comparison between two different methods in deriving  $C_D$  for pure wave and combined current-wave flows. The obtained insights can be valuable to the understanding and modelling of the wave-current-vegetation interactions. To achieve these goals, we re-analyze the data from recent lab experiments that measured  $WDV$  in both wave-only or combined wave-current conditions (Hu et al., 2014; Jadhav et al., 2013; Losada et al., 2016a,b; Ozeren et al., 2014). Both calibration and direct measurement methods are applied for comparison. To compare the different  $C_D$  deriving methods, we create a unique re-visiting procedure, which evaluates how well the derived  $C_D$  can reproduced the measured wave reduction and acting force. Finally, a synthesis of these two methods and a generic  $C_D$ -KC relation for both wave-only and combined wave-current flows is provided.

## 2. Methods

### 2.1. Data collection

To derive  $C_D$  via different methods and a  $C_D$ -KC relation in combined wave-current flow, we collected the published data of a recent experiments (Hu et al., 2014). The data of Hu et al. (2014) are analyzed in detail because velocity and acting force data were measured simultaneously at 1000 Hz, enabling the direct measurement method.

The experiment in Hu et al., (2014) was conducted in a wave flume with a 6 m long mimicked vegetation patch was placed in the middle of the wave flume (Fig. 2). The vegetation mimics were wooden cylinders with a diameter of 10 mm. The built vegetation canopy was 0.36 m tall and the tested water depths were 0.25 m and 0.50 m, respectively. The submergence ratio ( $h/h_v = 1-1.39$ ) is relatively small (Nepf, 2004). Regular waves are used in this test. The data of wave height, velocity and acting force in this previous study is collected in the current study to derive a new  $C_D$ -KC relation. The impact velocity data at locations 1–4 were measured by EMFs (electromagnetic flow meters). At locations 1 and 3, the acting force on vegetation mimics was measured by force sensors developed at Deltares (former Delft Hydraulics, The Netherlands). At locations 2 and 4, the force was measured by load cells (model 300) developed by UIILCELL. However, the cells at location 2 and 4 were not functioning properly during the experiment. Thus, only the force data measured at locations 1 and 3 are included in the current study. Hu et al. (2014) tested the conditions when steady currents flowed in the same direction as wave propagation, i.e. following current condition, while Losada et al. (2016a,b) tested conditions with both following and opposing currents. Current study is constrained to conditions with following currents only for parallel comparison.

Besides the above-mentioned two previous studies on combined current-wave flows,  $C_D$ -KC relations derived previously in Jadhav et al. (2013) and Ozeren et al. (2014) for wave-only conditions are also collected to be compared with the new relations derived in the current study. Ozeren et al. (2014) use rigid circular cylinders, with a diameter of 0.0094 m, a stem density  $N=156$  stems/ $m^2$  and a stem height  $h_v=0.63$  m, which is comparable to the experimental condition of this study. Jadhav et al. (2013) collected field data of  $WDV$  during a tropical storm, and the tested vegetation was flexible saltmarsh plants, *Spartina alterniflora*. The average stem density was  $N=422$  stems/ $m^2$  and the stem height was  $h_v=0.22$  m, while total plant height is 0.63 m and the averaged diameter of circular cylinder is determined as 0.008 m.

### 2.2. Data analysis

#### 2.2.1. Definition of KC and Re

The Keulegan Carpenter number  $KC$  is defined as:

$$KC = U_m T / b_v \quad (1)$$

where  $U_m$  is the measured maximum horizontal velocity in the wave propagation direction at the half water depth in both wave-only and wave-current flows. This velocity is chosen following Hu et al. (2014) because velocity at the half of the water depth roughly equals to the depth-average velocity in the vegetation canopy when the submergence ratio is small (e.g.  $h/h_v = 1-1.39$  in Hu et al. 2014). Thus, it is a good representative of the acting velocity on vegetation stems for conditions with small submergence ratios, and a suitable characteristic velocity for  $KC$  and  $Re$  definition.  $T$  is wave period and  $b_v$  is diameter of the circular cylinder, which is the common characteristic length for  $KC$  and  $Re$  in vegetated flow (Nepf, 2012). For real vegetation cases, the measured mean diameter of vegetation stems can be used as the characteristic length (Jadhav et al., 2013).  $Re$  is defined as:

$$Re = U_m b_v / \nu \quad (2)$$

$\nu$  being the kinematic viscosity of the fluid.

#### 2.2.2. Velocity data analysis

Considering Doppler Effect, the horizontal flow velocity in combined waves and current flow is given as:

$$U_{wc} = U_0 + \frac{gk}{2\sigma_{wc}} H \frac{\cosh k(z+h)}{\cosh kh} \cos(kx - \sigma t) \quad (3)$$

where  $U_0$  is unidirectional current velocity,  $g$  is the gravitational acceleration,  $\sigma_{wc}$  is the angular frequency associated with combined waves and currents ( $\sigma_{wc} = \sigma - U_0 k$ ),  $\sigma$  is angular frequency,  $k$  is the wave number,  $H$  is wave height and  $h$  is water depth. The subscript  $wc$  indicates the case of combined waves and currents.  $U_{wc}$  is the measured combined velocity at the half water depth, as it roughly equals to the depth-average velocity in the vegetation canopy, i.e. the acting velocity on vegetation.

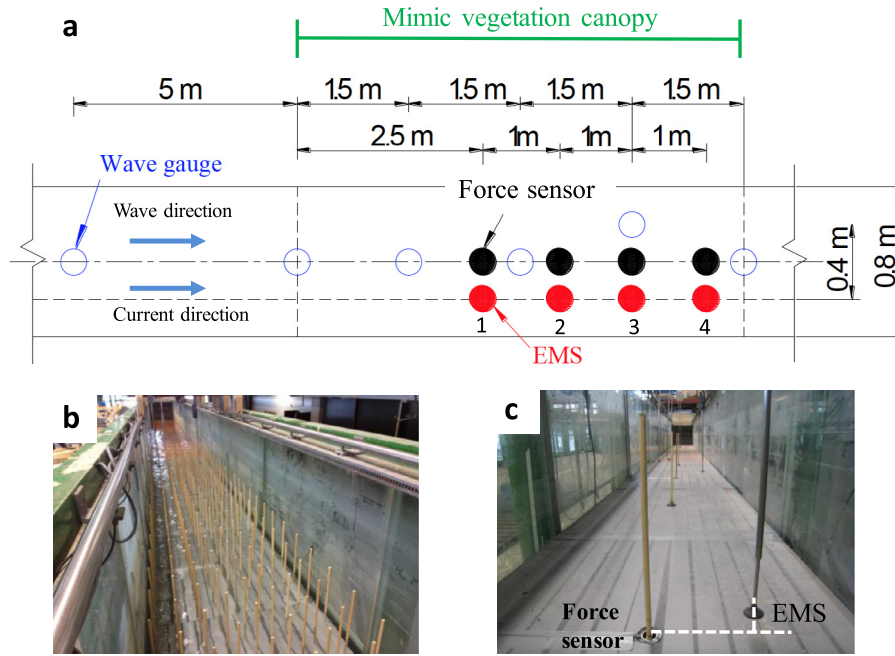


Fig. 2. Experiment set-up of Hu et al. (2014) to measure synchronized flow velocity ( $U_{wc}$ ) and acting force ( $F$ ) on wooden cylinders (mimic vegetation) at locations 1–4. (a) is the top view of the instruments and the mimic vegetation deployment. (b) is a photo of the constructed the mimic vegetation. (c) is a photo of synchronized force and velocity measurement to obtain in-phase data. The white dash lines indicate two instruments are placed at the same cross-section.

### 2.2.3. Deriving $C_{D,cal}$ in combined wave-current flows by calibration method

This section describes the derivation of  $C_{D,cal}$  in combined current-wave flow by calibration method following Losada et al. (2016a,b). It is only until recently the calibration approach has been extended to combined wave-current flows, as most previous models do not account for the effect of currents on WDV. Losada et al. (2016a,b) modified the analytical formulation of Dalrymple et al. (1984) to include the effect of currents on WDV  $C_{D,cal}$  in combined wave-current flows can be derived as:

$$C_{D,cal} = \left[ g \left( 1 + \frac{2kh}{\sinh 2kh} \right) \left( \frac{g}{k} \tanh kh \right)^{1/2} + gU_0 \left( 3 + \frac{4kh}{\sinh 2kh} \right) + 3kU_0^2 \left( \frac{g}{k} \coth kh \right)^{1/2} \right] \beta / \left[ \frac{16}{3\pi} N h_v b_v \left( \frac{gk}{2\sigma_{wc}} \right)^3 \frac{\sinh^3 kh_v + 3 \sinh kh_v}{3k \cosh^3 kh} H_0 \right] \quad (4)$$

where  $\beta$  is a damping coefficient stemmed from relative wave height ( $K_v$ ) attenuation in Dalrymple et al. (1984):

$$K_v = \frac{H}{H_0} = \frac{1}{1 + \beta x} \quad (5)$$

where  $H$  is the wave height along the vegetation mimic area and  $H_0$  is the initial wave height. When spatial wave height data are available,  $\beta$  can be obtained by fitting the Eq. (5). Subsequently, the obtained  $\beta$  can be substituted in Eq. (4) to derive  $C_{D,cal}$ .

### 2.2.4. Deriving $C_{D,dir}$ in combined wave-current flows by direct measurement method

In both pure wave and combined wave-current flows, force on a single stem can be expressed by Morison equation (Morison et al., 1950):

$$F = F_D + F_M = \frac{1}{2} \rho C_{D,dir} h_v b_v U |U| + \frac{\pi}{4} \rho C_M h_v b_v^2 \frac{\partial U}{\partial t} \quad (6)$$

where  $F$  is the total inline force on a vegetation stem,  $F_D$  is drag force,  $F_M$  is inertia force,  $\rho$  is the density of the fluid,  $C_{D,dir}$  and  $C_M$  are the drag

derived by direct measurement method and inertia coefficients respectively,  $h_v$  is the height of vegetation in water,  $b_v$  is the diameter of circular cylinder and  $U$  is horizontal flow velocity.

The direct measurement method derives  $C_{D,dir}$  from the perspective of the acting force on the vegetation cylinders. The period-averaged  $C_{D,dir}$  is derived by computing the work done by the total force over one period. It is assumed that the work done by  $F_M$  is zero or close to zero over a full wave period, and it holds for both wave-only and combined wave-current flows (Hu et al., 2014). Therefore, the work done by  $F_D$  is equal to the work done by the total force ( $F_{wc}$ ). Thus, a period-averaged drag coefficient can be derived from the following equation (Hu et al., 2014):

$$C_{D,dir} = \frac{2 \int_0^T F_D U_{wc} dt}{\int_0^T \rho h_v b_v U_{wc}^2 |U_{wc}| dt} = \frac{2 \int_0^T F U_{wc} dt}{\int_0^T \rho h_v b_v U_{wc}^2 |U_{wc}| dt} \quad (7)$$

where the total force  $F$  and  $U_{wc}$  can be directly obtained from actual measurements to derive  $C_{D,dir}$ . By applying Eq. (7), it is not necessary to separate  $F_D$  and  $F_M$  when deriving period-averaged drag coefficient. Accurately separating these two forces can be difficult because both forces are related to an unknown coefficient, i.e.  $C_D$  and  $C_M$ , and have different phase relations with the velocity. Additionally, this equation is applicable in both wave-only and combined wave-current conditions.

To check if it is valid to neglect the work done by  $F_M$  in Eq. (7), we quantify and compare the work done by  $F_D$  and  $F_M$ . The time-varying work done is evaluated as following:

$$\epsilon_D = F_D U_{wc} \quad (8)$$

$$\epsilon_M = F_M U_{wc} \quad (9)$$

where the time-varying  $F_D$  and  $F_M$  are obtained by separating the total measured force. We assume the inertia coefficient ( $C_M$ ) is 2 for cylinders (e.g. Dean and Dalrymple, 1991) and calculated the  $F_M$  following Eq. (6).  $F_D$  is then derived by subtracting  $F_M$  from the total force. Period-averaged work done by drag force ( $\epsilon_D$ ) and inertia force ( $\epsilon_M$ ) can be obtained by averaging the Eq. (8) and (9) over a full wave period.

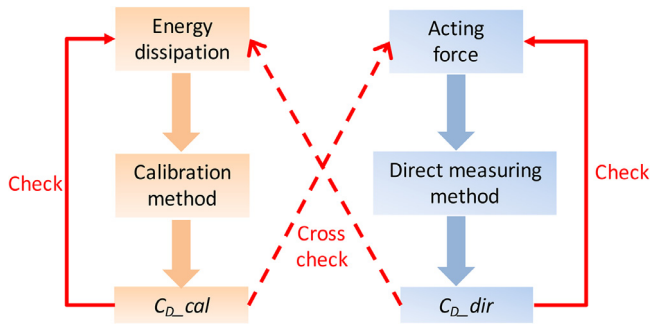


**Fig. 3.** The work flow of revisiting (checking) the derived drag coefficients by different methods. The calibration method derives  $C_{D,cal}$  from the perspective of wave energy dissipation, whereas the direct measurement method derives  $C_{D,dir}$  from the perspective of acting force on vegetation. We examine the derived drag coefficients by revisiting not only their directly linked quantities (i.e. energy dissipation or acting force, the solid red arrows), but also their counter parameters (the dash red arrows). (For interpretation of the references to colour in this figure legend, the reader is referred to the web version of this article.)

### 2.2.5. Revisiting the derived $C_D$

The calibration approach derives  $C_{D,cal}$  from the perspective of wave energy dissipation, whereas the direct measurement approach derives  $C_{D,dir}$  from the perspective of acting force. In order to provide an objective and quantitative evaluation of the two different methods, we revisit the derived drag coefficients following the procedure shown in Fig. 3. The derived drag coefficients by both methods are used to compute both the wave energy dissipation and the acting force. Thus, the derived drag coefficients were not only examined by their own linked quantity (energy dissipation or acting force) but also their counter quantity, providing a cross-check of the two different methods.

To check the validity of the derived  $C_{D,cal}$  and  $C_{D,dir}$  in reproducing WDV, they were used to compute  $\beta$  by reversing Eq. (4). The obtained  $\beta$  is then used in Eq. (5) to compute  $K_v$ , and subsequently compared with the measured  $K_v$  for evaluation. The reproduced  $K_v$  is denoted as  $K_{v,cal}$  when  $C_{D,cal}$  is used, and  $K_{v,dir}$  when  $C_{D,dir}$  is used. Similarly, to check the validity of  $C_{D,cal}$  and  $C_{D,dir}$  in reproducing acting force, they are utilized in Eq. (6) to reproduce both time-varying and the maximum total force, which are subsequently compared with the measurements. The reproduced maximum total force is denoted as  $F_{cal,max}$  and  $F_{dir,max}$ , respectively. It is expected that the WDV can be better reproduced by using  $C_{D,cal}$  and acting force can be better reproduced by using  $C_{D,dir}$ . These revisiting procedures are conducted to set a context for the cross-check: reproducing force with  $C_{D,cal}$  and reproducing WDV with  $C_{D,dir}$ . By combining both checks, we can evaluate which method can derive drag coefficients that have a better overall performance in reproducing both force and WDV.

## 3. Results

### 3.1. WDV and $C_D$ derived via calibration method

The calibration method derives  $C_{D,cal}$  based on spatial wave height reduction pattern, which can be influenced by co-existing currents. The wave height data in a recent studies (Hu et al., 2014) are shown in Fig. 4 to demonstrate the influence of co-existing currents on WDV and to illustrate how to calibrate  $C_{D,cal}$  values from the wave height data.

The experiment of Hu et al. (2014) shows that WDV can be either promoted or suppressed by a following current, depending on the (relative) magnitude of the current velocity (Fig. 4b). The WDV variations lead to different  $\beta$  values, and eventually are reflected in different  $C_{D,cal}$  values. The tested vegetation density was 139 stems/m<sup>2</sup>, and the tested mimics were 0.36 m tall (with 0.5 m water depth). The incident wave was regular wave with 0.08 m wave height and the wave period was

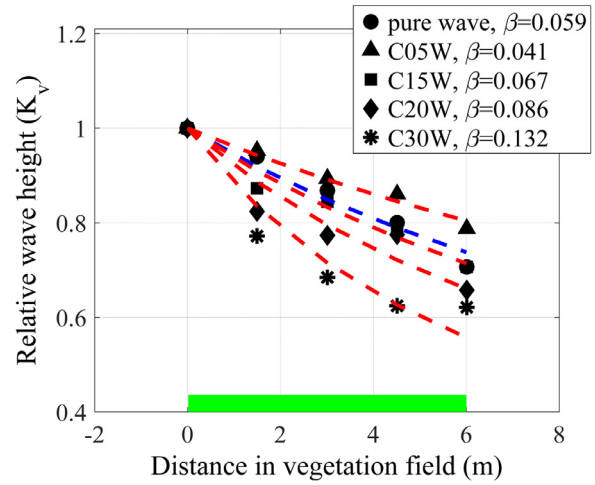


**Fig. 4.** The reduction of relative wave height ( $K_v$ ) along tested vegetation patches. The data were obtained in Hu et al. (2014). Test C05W means the wave with 0.05 m/s current velocity.

1.5 s. In wave-only conditions,  $\beta$  is fitted to be 0.059. With a small following current (0.05 m/s),  $\beta$  (and WDV) is reduced to be 0.041, but with larger following currents (0.15–0.30 m/s),  $\beta$  (and WDV) increases from 0.067 to 0.132, which is higher than that of the wave-only condition. The reason for the variation in WDV with different following current velocity magnitude is illustrated in Hu et al. (2014).

### 3.2. $C_{D,dir}$ derived via direct measurement method

The direct measurement method derives  $C_{D,dir}$  by calculating the work done by the total force acting on vegetation including both drag force ( $F_D$ ) and inertial force ( $F_M$ ) part (see Eq. 7). It is assumed that the work done by  $F_M$  is close to zero over a full wave period or much smaller comparing to that of  $F_D$ . Thus, it is not necessary to separate them while estimating the period-averaged  $C_{D,dir}$ . The relative magnitude of work done by  $F_D$  and  $F_M$  is therefore of importance to such assumption.

The work done by  $F_D$  and  $F_M$  over two wave period are shown in Fig. 5. The water level rigid plant mimic density and wave conditions are the same, and the current velocity increases from Fig. 5a to d. The temporally varying  $\epsilon_D$  and  $\epsilon_M$  have clear cyclic behaviors.  $\epsilon_D$  is always positive, but  $\epsilon_M$  alternates between positive and negative values. With the increased following current velocity,  $\epsilon_D$  and the period-averaged  $\bar{\epsilon}_D$  becomes larger, whereas the net value of period-averaged  $\bar{\epsilon}_M$  remains close to zero. In all 4 cases,  $\bar{\epsilon}_D$  is sufficiently higher than  $\bar{\epsilon}_M$ . Thus, the work done by the total force in Eq. (7) is dominated by  $F_D$ , and the influence of  $\bar{\epsilon}_M$  is limited over a full wave period.

Fig. 6 summarizes all the cases tested in Hu et al. (2014), and shows  $\bar{\epsilon}_D$  is in general much larger compared to  $\bar{\epsilon}_M$ . It is clear that with the increase of  $KC$ ,  $\bar{\epsilon}_D$  increases, whereas  $\bar{\epsilon}_M$  remains close to zero. The ratio between the absolute  $\bar{\epsilon}_D$  and  $\bar{\epsilon}_M$  is smaller with small  $KC$  values (around 10). The smallest ratio between them is about 3, implying that the  $\bar{\epsilon}_D$  is always the bulk part of the work done by the total force. Thus, it is considered acceptable to derive  $C_{D,dir}$  via Eq. (7) without separating the respective contribution of  $F_D$  and  $F_M$ .

### 3.3. $C_D$ -KC relations in wave-only condition

We first derive drag coefficients in wave-only flows that are tested in Hu et al. (2014), as it is the condition investigated by most previous studies. It is clear that  $C_D$ -KC relation derived by the direct measurement method shares the same general pattern as those derived by the calibration method, i.e.  $C_D$  decreases with the increased  $KC$  (Fig. 7). Comparing to the calibration method, the  $C_D$ -KC relation from the direct measurement method leads to less scattering among different mimic

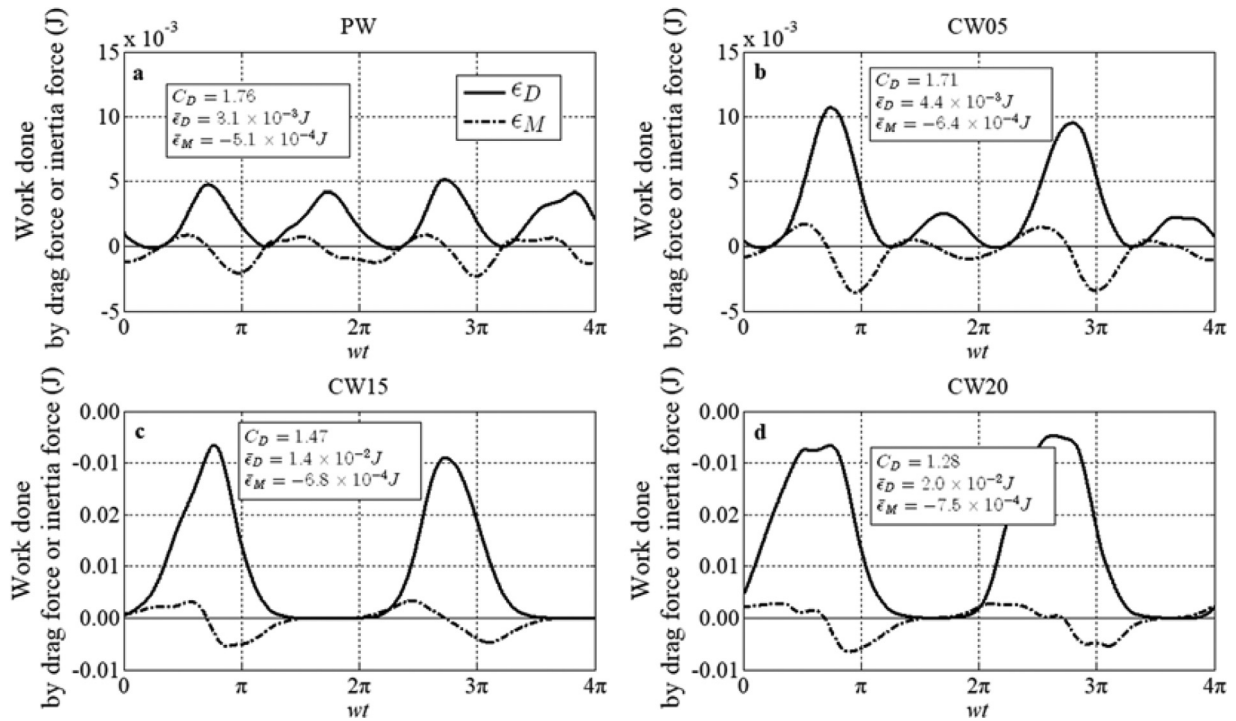


Fig. 5. Work done by acting drag force ( $\epsilon_D$ ) and inertia force ( $\epsilon_M$ ) in different hydrodynamic conditions; PW represents wave-only condition and C05W, C15W and C20W represent the wave with underlying current 0.05 m/s, 0.15 m/s and 0.20 m/s respectively.

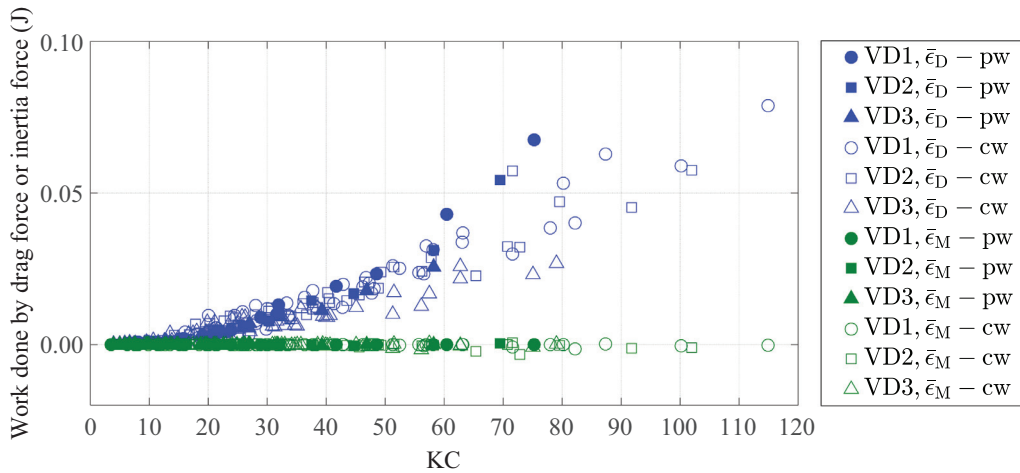


Fig. 6. The relation between  $KC$  number and the work done by drag force ( $\bar{\epsilon}_D$ ) or inertia force ( $\bar{\epsilon}_M$ ) over a wave period. ‘pw’ stands for wave-only conditions and ‘cw’ stands for current wave conditions.

densities and submergence conditions (Fig. 7c and d). Following the direct measurement approach, the  $C_D$ - $KC$  relation for pure wave cases is:

$$C_D = 6.94 * KC^{(-0.72)} + 0.87 (R^2 = 0.79) \quad (10)$$

It is noted that the above relation has much higher  $R^2$  value comparing to that derived by the calibration method ( $R^2=0.21$ ). Furthermore, the above relation is similar to the  $C_D$ - $KC$  relation proposed in Ozeren et al. (2014) (Fig. 7a), but different from that in Jadhav et al. (2013) (Fig. 7b). It is noted that the relation in Ozeren et al. (2014) is applicable when  $KC$  is in the range between 5 and 35, whereas the relation in Jadhav et al. (2013) is applicable when  $KC$  is in the range between 25 and 135.

### 3.4. $C_D$ - $KC$ relation in combined wave-current flows

By using the new model of Losada et al. (2016a,b), drag coefficients in combined current-wave flows can also be derived by the calibration method. Previously, they could only be derived by the direct measurement method. In Fig. 8, we compare the  $C_D$ - $KC$  relations derived by both methods. Both relations for combined wave-current flow have the general reduction trend similar to that in wave-only conditions. Because of the superimposed current  $U_0$ , the combined wave-current conditions were inherently associated with higher  $KC$ . As  $KC$  varies in the range between 7 and 120, the  $C_{D,cal}$  from the calibrated method reduces from 10.59 to 0.25. It is clear that  $C_{D,cal}$  has a substantial degree of scattering among different mimic stem densities and water depths. The degree of scattering is much reduced in the relation between  $C_{D,dir}$  and  $KC$



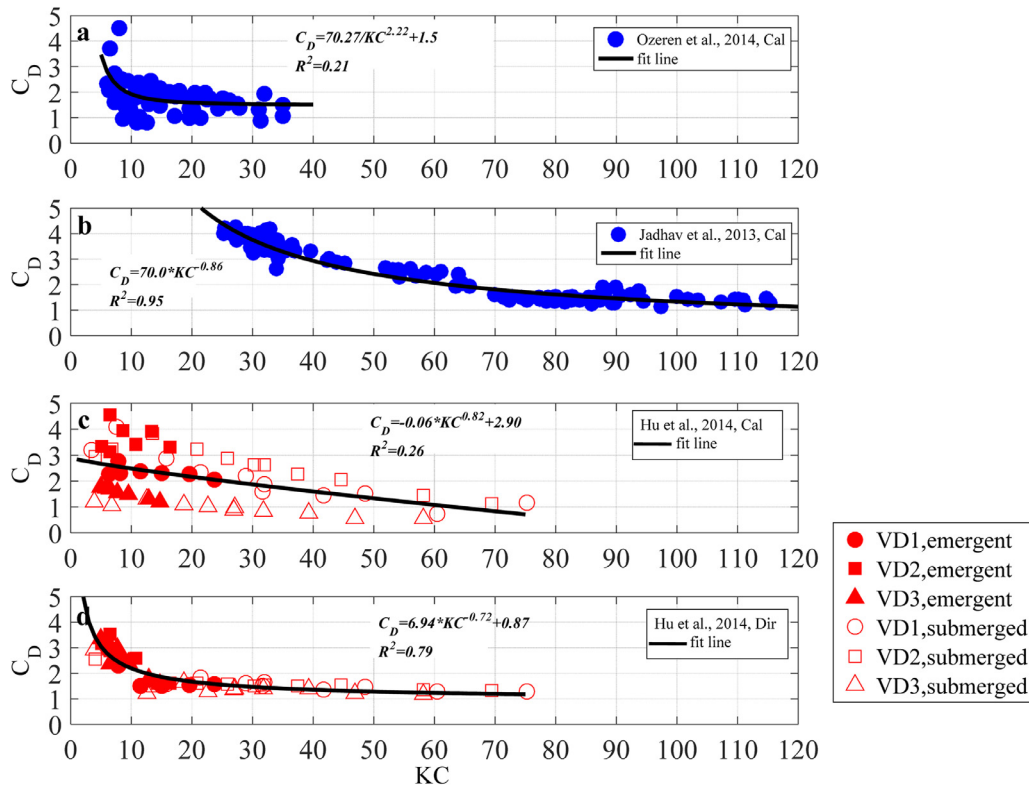


Fig. 7. Relation between  $KC$  and  $C_D$  based on various data source. (a) is based on calibrated  $C_D$  in Ozeren et al. (2014); (b) is based on calibrated  $C_D$  in Jadhav et al. (2013); (c) is based on calibrated  $C_D$  in Hu et al. (2014); (d) is based on  $C_D$  data that are derived by the direct measurement method in Hu et al. (2014).

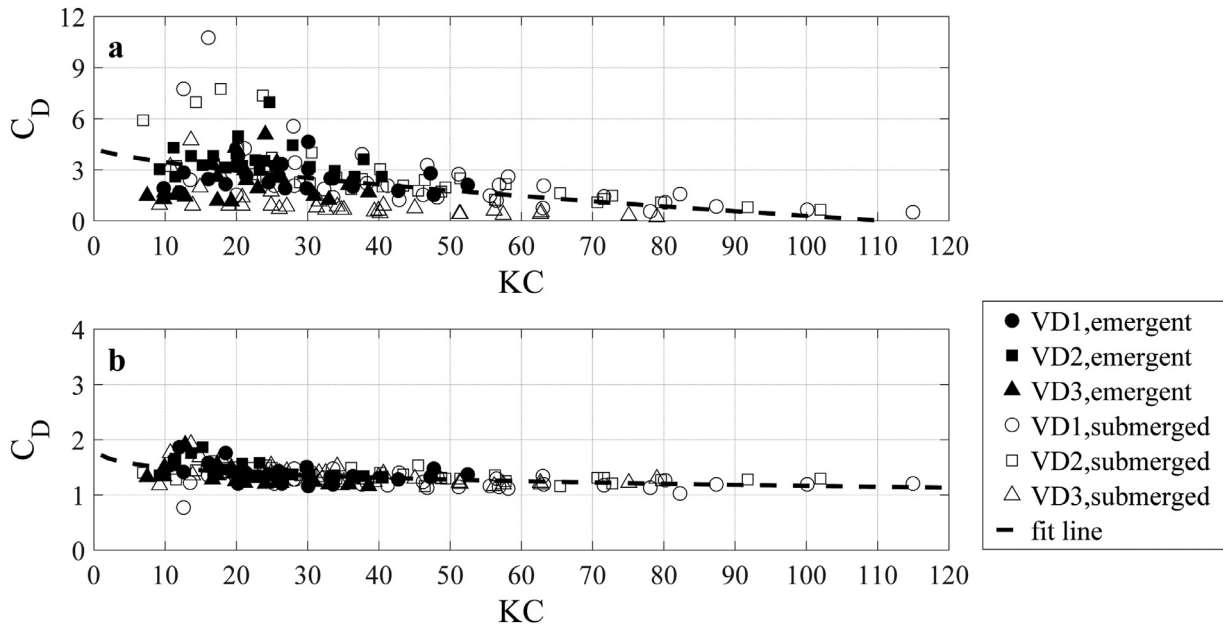


Fig. 8. Relation between  $KC$  and  $C_D$ ; panel a is derived by calibration method in combined wave-current flow; panel b is derived by direct measurement approach in combined wave-current flow.

(Fig. 8). The obtained  $C_{D,dir}$  is within the range of 1 to 2. No apparent difference between different densities and submergence ratio can be observed.

To obtain a generic relation for both wave-only conditions and combined wave-current conditions, we summarize all the  $C_{D,dir}$  from Hu et al. (2014) in Fig. 9. The  $C_D$ - $KC$  relation for both flows can be

expressed as:

$$C_D = 12.89 * KC^{(-1.25)} + 1.17 (R^2 = 0.66) \tag{11}$$

The above relation shows that in both wave-only conditions and combined wave-current conditions,  $C_D$ - $KC$  relation has a similar trend, i.e., with the increasing  $KC$ ,  $C_D$  gradually decreases and approaches to a constant value (i.e. 1.2). Furthermore, this empirical  $C_D$ - $KC$  relation

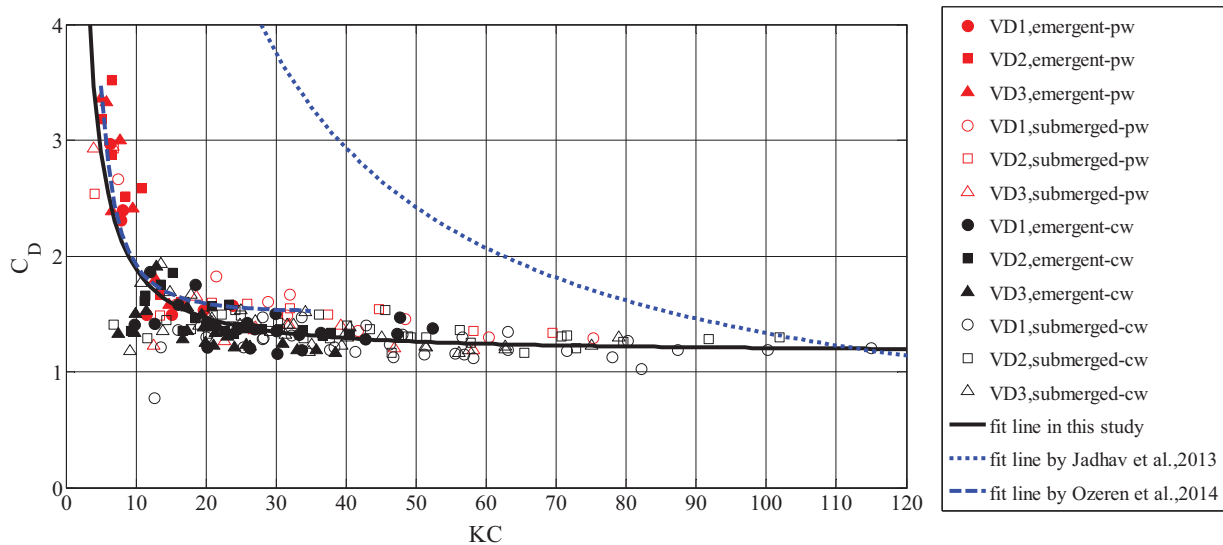


Fig. 9.  $C_D$ - $KC$  relation in both wave-only and combined wave current conditions based on direct measurement method. The red markers and “pw” stand for the results of wave-only conditions, while the black markers and “cw” stands for the results of combined wave current conditions. the fit equation from Jadhav et al. (2013) and Ozeren et al. (2014), see Table 1.

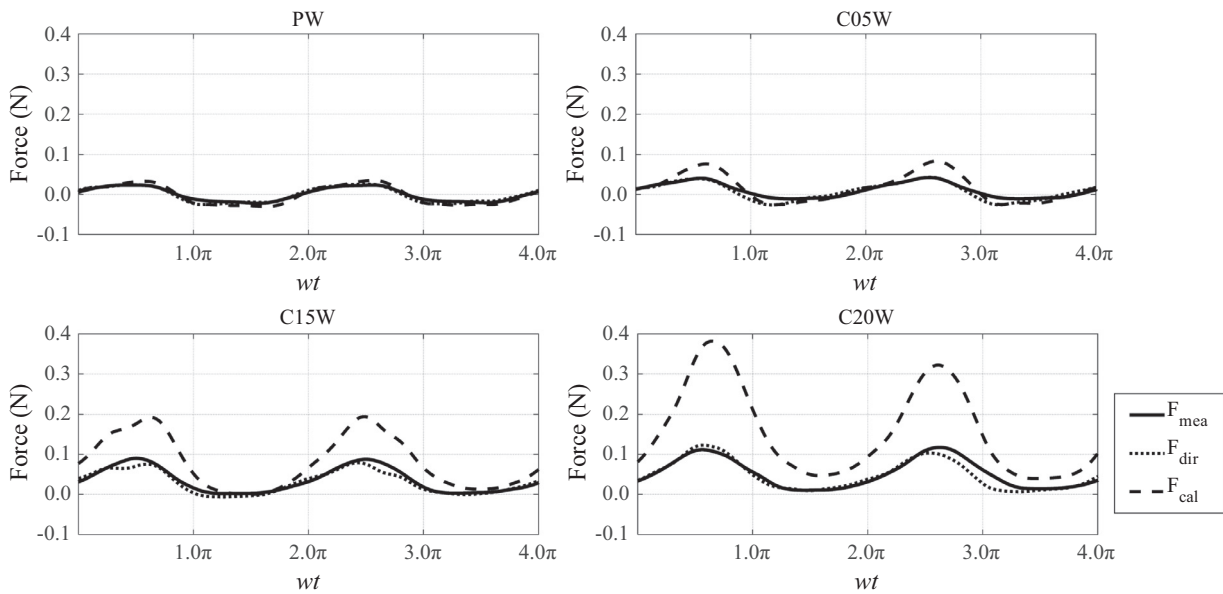


Fig. 10. Measured and reproduced total force acting on first force sensor (see Fig. 1) over two wave periods.

is similar to that in Ozeren et al. (2014), but different to that in Jadhav et al. (2013).

### 3.5. Revisiting the validity of the derived $C_{D-dir}$ and $C_{D-cal}$

To further test the applicability of the two different methods, the derived drag coefficients were revisited by using them to compute  $F$  as well the  $WDV$ . The computed force and wave decay are subsequently compared with the measurements. The computed (using Eq. (4)) and measured instantaneous total acting force is plotted in Fig. 10. With no or small following currents (PW and CW05 cases), the total force oscillates in between positive and negative directions. When the following currents becomes larger (CW15 and CW20), the total force stays in the positive directions for a full period. It is clear that the temporal variation of the total force calculated using  $C_{D-dir}$  ( $F_{dir}$ ) agrees well with

the measured total force, while as the total force calculated using  $C_{D-cal}$  ( $F_{cal}$ ) overestimates the total force when the following currents is strong. The shown data is from the test case with 6 cm wave height and 1.2 s wave period in Hu et al. (2014). The  $C_{D-dir}$  for the PW, CW05, CW10 and CW20 condition are 2.51, 1.76, 1.33 and 1.37, respectively. However, the  $C_{D-cal}$  for the same conditions are 3.94, 3.82, 3.53 and 4.46, which are considerably larger than  $C_{D-dir}$ . The maximum reproduced force over a wave period ( $F_{max,cal}$  and  $F_{max,dir}$ ) shown in Fig. 10 are further analyzed in the following section.

Fig. 11 shows the results of the cross-check process as demonstrated in Fig. 3. It is not surprising that good agreement can be obtained when check the derived  $C_{D-dir}$  and  $C_{D-cal}$  with their own linked quantities. The  $R^2$  value is 0.98 between  $F_{dir,max}$  (i.e. the maximum total force over one wave period computed using  $C_{D-dir}$ ) and the measured maximum total force ( $F_{mea,max}$ ) (data not show). Similarly, the  $R^2$  value is 0.99 be-

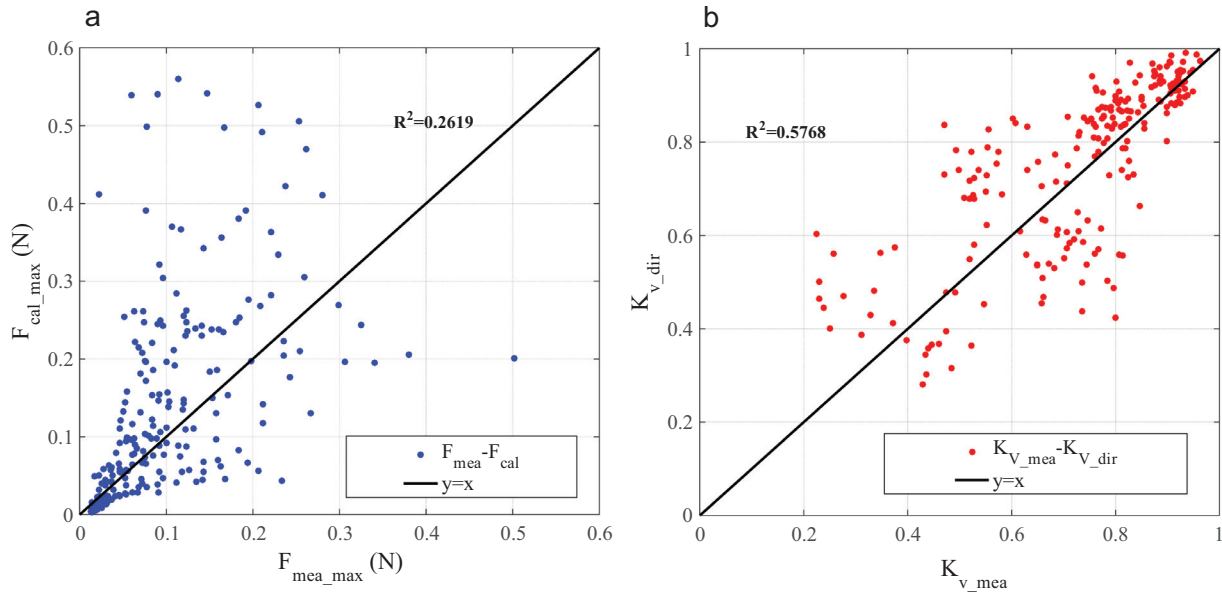


Fig. 11. (a) comparing reproduced maximum total force based on  $C_{D,cal}$  (i.e.  $F_{cal,max}$ ) with measured maximum total force ( $F_{mea,max}$ ), (b) comparing the reproduced relative wave height based on  $C_{D,dir}$  (i.e.  $K_{v,dir}$ ) with the measured relative wave height ( $K_{v,mea}$ ). The  $y=x$  lines are plotted for reference.

tween  $K_{v,cal}$  and  $K_{v,mea}$  (data not show). The cross-check process, however, provides us with future insights. It is clear that  $F_{cal,max}$  (i.e. the maximum total force over one wave period computed using  $C_{D-cal}$ ) does not match with  $F_{mea,max}$ . The corresponding  $R^2$  value is only 0.26. Similarly, the agreement between the  $K_{v,dir}$  (i.e.  $WDV$  computed using  $C_{D-dir}$ ) and  $K_{v,mea}$  is also not ideal. The resulting  $R^2$  value is 0.58. In summary, it is clear that the total force and  $WDV$  derived using  $C_{D-cal}$  have better overall agreement with measurements.

## 4. Discussion

### 4.1. $C_D$ - $KC$ relations in wave-only and combined wave-current conditions

In natural coastal wetlands, combined wave-current flows are common flow conditions. To our knowledge, existing  $C_D$ - $KC$  relations are all for vegetation in wave-only conditions, such relations whereas in combined wave-current conditions have not yet been derived. By reanalyzing the data of Hu et al. (2014), we derived a new overall  $C_D$ - $KC$  relation for both wave-only and combined wave-current flow conditions in the present study. This new relation retains the same general form as previous studies listed in Table 1. With increasing  $KC$  number, the  $C_D$  values decrease regardless of the flow conditions and gradually approach 1. The derived relation is of value to the understanding and modelling  $WDV$ .

$C_D$  has generally been expressed as functions of  $Re$ , and previous studies have derived  $C_D$ - $Re$  relations for pure current, wave-only and combined wave-current conditions (Hu et al., 2014). Previous studies have suggested that  $C_D$ - $KC$  relations are more suitable for oscillatory flows (Augustin et al., 2009; Mendez and Losada, 2004; Ozeren et al., 2014). Compared to  $Re$  that depends solely on maximum velocity,  $KC$  numbers contain additional information of wave period. Thus, they are expected to result in more suitable functions in describing  $C_D$  dynamics. However, the new  $C_D$ - $KC$  relation obtained here show otherwise. The  $R^2$  value of the derived new  $C_D$ - $KC$  relation (including both pure-wave and combined current-wave) is 0.66, which is lower compared to the  $R^2$  value (0.89) of the derived overall  $C_D$ - $Re$  relation in Hu et al. (2014). This may be attributed to the test vegetation mimics in Hu et al. (2014) were rigid sticks, whereas previous studies that obtained better  $C_D$ - $KC$  correlations generally tested flexible vegetation mimics (e.g. Augustin et al., 2009; Mendez and Losada, 2004; Ozeren et al., 2014). This indicates that the dependence of  $C_D$  on  $KC$  (wave

period) is stronger with flexible vegetation. Nonetheless, the derived  $C_D$ - $KC$  relation is of value to interpreting the  $WDV$  process. Our results confirm that in both wave-only and combined wave-current conditions, the variation of  $C_D$  with  $KC$  follows the same trend, which has not been reported before.

### 4.2. Comparing two different methods in deriving $C_D$

The current study derives the drag coefficients by two different approaches, aiming to compare them and provide guidelines for future experimental studies. Such a comparison was not possible until the recent model development that includes the effect of current into  $WDV$  modelling (Losada et al., 2016a,b). A detailed comparison of these two methods is included in the Table 2.

These two methods are compared in terms of their main equations, required data, flow conditions, applicable environments, the performances in reproducing force and  $WDV$ , as well as the  $R^2$  value of the  $C_D$ - $KC$  relations (Table 2). The calibration approach makes use of the energy dissipation equation and wave height data, whereas the direct measurement approach relies on Morrison equation and synchronized velocity and force data. Clearly, the  $C_D$ - $KC$  relation derived by the direct measurement method have considerably higher  $R^2$  value than that derived by the calibration method (Figs. 7 and 8). However, the calibration approach has a wider range of application, as it can be applied in both lab and field environments. With the current instrumentation, the direct measurement method is only applicable in lab conditions, as it requires synchronized force and velocity data with high accuracy, which are not feasible to obtain in field conditions. Additionally, the calibration methods can be readily used in flexible vegetation cases (Maza et al., 2015b; Lara et al., 2016; I.J. Losada et al., 2016a,b), whereas the direct measurement method is not yet able to do so. It is because such method requires measurement of acting velocity on vegetation stem, i.e. relative velocity between water motion and vegetation stem motion, which is difficult to measure with the current setup. However, it is possible if the video analysis technique is included for relative velocity measurements (Luhar and Nepf, 2016).

The calibration method derives  $C_D$  from the perspective of wave energy dissipation, whereas the direct measurement method is from the perspective of vegetation-induced force. In order to evaluate these two methods objectively, we used the derived  $C_D$  from the different methods

**Table 2**  
Comparison of two approaches in determining  $C_D$ .

	Calibration approach	Direct measurement approach
<b>References</b>	Dalrymple et al., 1984; Kobayashi et al., 1993; Losada et al., 2016a,b; Mendez and Losada, 2004; Möller et al., 2014	Hu et al., 2014; Infantes et al., 2011
<b>Main equation</b>	Wave height reduction by vegetation <sup>a</sup> : $C_D = \left[ g \left( 1 + \frac{2kh}{\sinh 2kh} \right) \left( \frac{g}{k} \tanh kh \right)^{1/2} + gU_0 \left( 3 + \frac{4kh}{\sinh 2kh} \right) + 3kU_0^2 \left( \frac{g}{k} \coth kh \right)^{1/2} \right]$ $\beta / \left[ \frac{16}{3\pi} N b_c \left( \frac{gk}{2\sigma_{wc}} \right)^3 \frac{\sinh^3 kh_c + 3 \sinh kh_c}{3k \cosh^3 kh} H_0 \right]$	Morrison equation: $C_D = \frac{2 \int_0^T F U_{wc} dt}{\int_0^T \rho h_c b_c U_{wc}^2  U_{wc}  dt}$
<b>Required data</b>	Wave height spatial distribution	Synchronized impact flow velocity ( $U_{wc}$ ) and acting force ( $F$ ) on vegetation cylinders
<b>Flow conditions</b>	Wave-only and combined wave-current flow	Wave-only, pure current and combined wave-current flow
<b>Applicable environment</b>	Laboratory and field	Laboratory
<b>Applicable vegetation</b>	Rigid and flexible vegetation	Rigid vegetation
<b>R<sup>2</sup> value when revisiting acting Force<sup>b</sup></b>	0.26	0.98
<b>R<sup>2</sup> value when revisiting <math>K_v</math><sup>c</sup></b>	0.99	0.58
<b>R<sup>2</sup> value of <math>C_D</math>-<math>KC</math> relations<sup>d</sup></b>	0.19 ( $C_D = -0.024 * KC^{-1.05} + 3.26$ )	0.66 ( $C_D = 12.89 * KC^{-1.25} + 1.17$ )

<sup>a</sup> The listed equation is the recent formulations derived in Losada et al. (2016a,b) for combined current and wave flows. It should be noted that a variety of equations exist in calibrating  $C_D$ , depending on the applied wave decay model.

<sup>b, c, d</sup> The comparison is based on the data in Hu et al. (2014).

to compute both the acting force and the *WDV*. Thus, providing a cross-examination of these two methods (Fig. 3). We show that the  $C_D$  values derived from the perspective of force can better reproduce the measured force ( $R^2 = 0.98$ ) compared to  $C_{D-cal}$  ( $R^2 = 0.26$ ). However, the  $C_D$  values of the direct measurement method perform poorer in reproducing *WDV* ( $R^2 = 0.58$ ) compared to that of  $C_{D-cal}$  ( $R^2 = 0.99$ ). Therefore, the  $C_D$  derived from either energy or force perspective can fit better with their own respective quantity but not the counter quantity as shown in Fig. 11.

The reason that different methods leads to different  $C_D$  values is perhaps that the work done by the drag force is not the only process leading to *WDV*. Other processes like turbulence as well as surface friction of vegetation mimics and flume walls also contribute to energy dissipation, but they are not accounted in the current *WDV* models. Thus, the derived  $C_{D-cal}$  is actually a synthesis for a number of processes, whereas  $C_{D-dir}$  is only responsible for acting force. Because of the involvement of the additional processes, the  $C_{D-cal}$  and  $C_{D-dir}$  do not provide the same performance in the cross-check as the check with their own respective measurements (see Fig. 3). Overall, the check of  $C_{D-dir}$  obtains better agreement with measured acting force ( $R^2 = 0.98$ ) and *WDV* ( $R^2 = 0.58$ ). The revisiting procedure also imply that numerical models that are built upon momentum conservation equations should seek to use the  $C_{D-dir}$ , whereas other models that rely on energy conservation (and do not explicitly account for turbulence and friction effects) should use  $C_{D-cal}$  for better simulations of *WDV* process.

### 5. Conclusions

By re-analyzing the previous data of Hu et al. (2014), this study aims to reduce the uncertainties in the different  $C_D$  deriving methods and the dependence of  $C_D$  on hydrodynamic parameters (i.e. *Re* and *KC*). The two available methods in deriving  $C_D$ , i.e. the direct measurement method and the calibration method, are compared in terms of their main equations, required data, flow conditions, applicable environments, and

the resulting  $C_D$ -*KC* relations (Table 2). Furthermore, we create a unique re-visiting procedure, which evaluates how well the derived drag coefficients can be used to reproduce the measured wave reduction and acting force. To our knowledge, current study is the first study providing a thorough comparison between these two methods, which may assist experiment design for further investigation of  $C_D$ .

Additionally, we formulate a new empirical relation between  $C_D$  and *KC* as an extension to the  $C_D$ -*Re* relation in Hu et al. (2014). The  $C_D$ -*KC* relation is based on the direct measurement method, and it is a generic relation for both wave-only and combined wave-current conditions. The derived  $C_D$ -*KC* relation for both wave-only and combined wave-current conditions have a similar decreasing trend as previous relations for wave-only cases, which has not been reported previously. The obtained generic  $C_D$ -*KC* relation is expected to be useful to future numerical modeling studies.

### Acknowledgements

The authors thank two anonymous reviewers and an Editorial Board member for their comments that helped to improve this paper. The authors gratefully acknowledge financial support of the National Natural Science Foundation of China (No. 51609269, 51520105014), and the Joint Research Projects NSFC (No. 51761135022) – NWO (No. ALWSD.2016.026) – EPSRC (No. EP/R024537/1): Sustainable Deltas, and Science and Technology Program of Guangzhou City, China (201806010143).

### Supplementary materials

Supplementary material associated with this article can be found, in the online version, at doi:10.1016/j.advwatres.2018.10.008.

### References

Anderson, M.E., Smith, J.M., 2014. Wave attenuation by flexible, idealized salt marsh vegetation. *Coast. Eng.* 83, 82–92. <https://doi.org/10.1016/j.coastaleng.2013.10.004>.

- Anderson, M.E., Smith, J.M., McKay, S.K., 2011. Wave dissipation by vegetation. ERDC CHETN-82.
- Arkema, K.K., Guannel, G., Verutes, G., Wood, S.A., Guerry, A., Ruckelshaus, M., Kareiva, P., Lacayo, M., Silver, J.M., 2013. Coastal habitats shield people and property from sea-level rise and storms. *Nat. Clim. Change* 3, 913–918. <https://doi.org/10.1038/nclimate1944>.
- Augustin, L.N., Irish, J.L., Lynett, P., 2009. Laboratory and numerical studies of wave damping by emergent and near-emergent wetland vegetation. *Coast. Eng.* 56, 332–340. <https://doi.org/10.1016/j.coastaleng.2008.09.004>.
- Bouma, T.J., De Vries, M.B., Low, E., Peralta, G., Tanczos, I.C., Van De Koppel, J., Herman, P.M.J., 2005. Trade-offs related to ecosystem engineering: a case study on stiffness of emerging macrophytes. *Ecology* 86, 2187–2199.
- Bradley, K., Houser, C., 2009. Relative velocity of seagrass blades: Implications for wave attenuation in low-energy environments. *J. Geophys. Res. F Earth Surf* 114.
- Cao, H., Feng, W., Hu, Z., Suzuki, T., Stive, M.J.F., 2015. Numerical modeling of vegetation-induced dissipation using an extended mild-slope equation. *Ocean Eng* 110, 258–269. <https://doi.org/10.1016/j.oceaneng.2015.09.057>.
- D'Alpaos, A., Marani, M., 2016. Reading the signatures of biologic–geomorphic feedbacks in salt-marsh landscapes. *Adv. Water Resour.* 93 (Part B), 265–275. Ecogeomorphological feedbacks of water fluxes, sediment transport and vegetation dynamics in rivers and estuaries <https://doi.org/10.1016/j.advwatres.2015.09.004>.
- D'Alpaos, A., Toffolon, M., Camporeale, C., 2016. Ecogeomorphological feedbacks of water fluxes, sediment transport and vegetation dynamics in rivers and estuaries. *Adv. Water Resour.* 93 (Part B), 151–155. Ecogeomorphological feedbacks of water fluxes, sediment transport and vegetation dynamics in rivers and estuaries <https://doi.org/10.1016/j.advwatres.2016.05.019>.
- Dalrymple, R.A., Kirby, J.T., Hwang, P.A., 1984. Wave diffraction due to areas of energy dissipation. *J. Waterw. Port Coast. Ocean Eng. ASCE* 110, 67–79. [https://doi.org/10.1061/\(ASCE\)0733-950X\(1984\)110:1\(67\)](https://doi.org/10.1061/(ASCE)0733-950X(1984)110:1(67)).
- Dean, R., Dalrymple, R., 1991. *Water Wave Mechanics for Engineers and Scientists, Advanced Series on Ocean Engineering*. World Scientific, Tokyo.
- Donnelly, J.P., Cleary, P., Newby, P., Ettinger, R., 2004. Coupling instrumental and geological records of sea-level change: evidence from southern New England of an increase in the rate of sea-level rise in the late 19th century. *Geophys. Res. Lett.* 31. L05203 <https://doi.org/10.1029/2003GL018933>.
- Fonseca, M.S., Cahalan, J.A., 1992. A preliminary evaluation of wave attenuation by four species of seagrass. *Estuar. Coast. Shelf Sci.* 35, 565–576. [https://doi.org/10.1016/S0272-7714\(05\)80039-3](https://doi.org/10.1016/S0272-7714(05)80039-3).
- Henry, P.Y., Myrhaug, D., Aberle, J., 2015. Drag forces on aquatic plants in nonlinear random waves plus current. *Estuar. Coast. Shelf Sci.* 165, 10–24. <https://doi.org/10.1016/j.ecss.2015.08.021>.
- Hu, Z., Suzuki, T., Zitman, T., Uittewaal, W., Stive, M., 2014. Laboratory study on wave dissipation by vegetation in combined current-wave flow. *Coast. Eng.* 88, 131–142. <https://doi.org/10.1016/j.coastaleng.2014.02.009>.
- Infantes, E., Orfila, A., Bouma, T.J., Simarro, G., Terrados, J., 2011. *Posidonia oceanica* and *Cymodocea nodosa* seedling tolerance to wave exposure. *Limnol. Oceanogr* 56, 2223–2232. <https://doi.org/10.4319/lo.2011.56.6.2223>.
- Jadhav, R.S., Chen, Q., Smith, J.M., 2013. Spectral distribution of wave energy dissipation by salt marsh vegetation. *Coast. Eng.* 77, 99–107. <https://doi.org/10.1016/j.coastaleng.2013.02.013>.
- Kobayashi, N., Raichle Andrew, W., Toshiyuki, Asano, 1993. Wave attenuation by vegetation. *J. Waterw. Port Coast. Ocean Eng.* 119, 30–48. [https://doi.org/10.1061/\(ASCE\)0733-950X\(1993\)119:1\(30\)](https://doi.org/10.1061/(ASCE)0733-950X(1993)119:1(30)).
- Lara, J.L., Maza, M., Ondiviela, B., Trinogga, J., Losada, I.J., Bouma, T.J., Godejuela, N., 2016. Large-scale 3-D experiments of wave and current interaction with real vegetation. Part 1: guidelines for physical modeling. *Coast. Eng.* 107, 70–83. <https://doi.org/10.1016/j.coastaleng.2015.09.012>.
- Li, C.W., Yan, K., 2007. Numerical investigation of wave-current-vegetation interaction. *J. Hydraul. Eng.* 133, 794–803. [https://doi.org/10.1061/\(ASCE\)0733-9429\(2007\)133:7\(794\)](https://doi.org/10.1061/(ASCE)0733-9429(2007)133:7(794)).
- Losada, InigoJ., Maza, M., Lara, J.L., 2016a. A new formulation for vegetation-induced damping under combined waves and currents. *Coast. Eng.* 107, 1–13. <https://doi.org/10.1016/j.coastaleng.2015.09.011>.
- Losada, I.J., Maza, M., Lara, J.L., 2016b. A new formulation for vegetation-induced damping under combined waves and currents. *Coast. Eng.* 107, 1–13. <https://doi.org/10.1016/j.coastaleng.2015.09.011>.
- Luhar, M., Infantes, E., Nepf, H., 2017. Seagrass blade motion under waves and its impact on wave decay. *J. Geophys. Res.-Oceans* 122, 3736–3752. <https://doi.org/10.1002/2017JC012731>.
- Luhar, M., Nepf, H.M., 2013. From the blade scale to the reach scale: a characterization of aquatic vegetative drag. *Adv. Water Resour.* 51, 305–316. <https://doi.org/10.1016/j.advwatres.2012.02.002>.
- Luhar, M., Nepf, H.M., 2016. Wave-induced dynamics of flexible blades. *J. Fluids Struct.* 61, 20–41. <https://doi.org/10.1016/j.jfluidstructs.2015.11.007>.
- Maza, M., Lara, J.L., Losada, I.J., 2015a. Tsunami wave interaction with mangrove forests: a 3-D numerical approach. *Coast. Eng.* 98, 33–54. <https://doi.org/10.1016/j.coastaleng.2015.01.002>.
- Maza, M., Lara, J.L., Losada, I.J., 2013. A coupled model of submerged vegetation under oscillatory flow using Navier-Stokes equations. *Coast. Eng.* 80, 16–34. <https://doi.org/10.1016/j.coastaleng.2013.04.009>.
- Maza, M., Lara, J.L., Losada, I.J., Ondiviela, B., Trinogga, J., Bouma, T.J., 2015b. Large-scale 3-D experiments of wave and current interaction with real vegetation. Part 2: experimental analysis. *Coast. Eng.* 106, 73–86. <https://doi.org/10.1016/j.coastaleng.2015.09.010>.
- Méndez, F.J., Losada, I.J., 2004. An empirical model to estimate the propagation of random breaking and nonbreaking waves over vegetation fields. *Coast. Eng.* 51, 103–118.
- Mendez, F.J., Losada, I.J., 2004. An empirical model to estimate the propagation of random breaking and nonbreaking waves over vegetation fields. *Coast. Eng.* 51, 103–118. <https://doi.org/10.1016/j.coastaleng.2003.11.003>.
- Mendez, F.J., Losada, I.J., Losada, M.A., 1999. Hydrodynamics induced by wind waves in a vegetation field. *J. Geophys. Res.-Oceans* 104, 18383–18396. <https://doi.org/10.1029/1999JC900119>.
- Méndez, F.J., Losada, I.J., Losada, M.A., 1999. Hydrodynamics induced by wind waves in a vegetation field. *J. Geophys. Res. C Oceans* 104, 18383–18396.
- Möller, I., Kudella, M., Rupprecht, F., Spencer, T., Paul, M., van Wesenbeeck, B.K., Wolters, G., Jensen, K., Bouma, T.J., Miranda-Lange, M., Schimmels, S., 2014. Wave attenuation over coastal salt marshes under storm surge conditions. *Nat. Geosci.* 7, 727–731. <https://doi.org/10.1038/NGeo2251>.
- Morison, J.R., Johnson, J.W., Schaaf, S.A., 1950. The force exerted by surface waves on piles. *J. Pet. Technol.* 2, 149–154. <https://doi.org/10.2118/950149-G>.
- Nepf, H., 2012. Flow Over and Through Biota. *Treatise on Estuarine and Coastal Science*, pp. 267–287. <https://doi.org/10.1016/B978-0-12-374711-2.00213-8>.
- Nepf, H.M., 2004. Vegetated flow dynamics. In: Fagherazzi, S., Marani, M., Blum, L.K. (Eds.), *Coastal and Estuarine Studies*. American Geophysical Union, Washington, D. C., pp. 137–163.
- Nepf, H.M., 1999. Drag, turbulence, and diffusion in flow through emergent vegetation. *Water Resour. Res.* 35, 479–489. <https://doi.org/10.1029/1998WR900069>.
- Ozereen, Y., Wren, D.G., Wu, W., 2014. Experimental investigation of wave attenuation through model and live vegetation. *J. Waterw. Port Coast. Ocean Eng.* 140. 04014019 [https://doi.org/10.1061/\(ASCE\)JWW.1943-5460.0000251](https://doi.org/10.1061/(ASCE)JWW.1943-5460.0000251).
- Paul, M., Bouma, T.J., Amos, C.L., 2012. Wave attenuation by submerged vegetation: combining the effect of organism traits and tidal current. *Mar. Ecol. Prog. Ser.* 444, 31–41. <https://doi.org/10.3354/meps09489>.
- Paul, M., Rupprecht, F., Möller, I., Bouma, T.J., Spencer, T., Kudella, M., Wolters, G., van, W., Jensen, K., Miranda-Lange, M., Schimmels, S., 2016. Plant stiffness and biomass as drivers for drag forces under extreme wave loading: a flume study on mimics. *Coast. Eng.* 117, 70–78. <https://doi.org/10.1016/j.coastaleng.2016.07.004>.
- Suzuki, T., Zijlema, M., Burger, B., Meijer, M.C., Narayan, S., 2012. Wave dissipation by vegetation with layer schematization in SWAN. *Coast. Eng.* 59, 64–71. <https://doi.org/10.1016/j.coastaleng.2011.07.006>.
- Temmerman, S., Kirwan, M.L., 2015. Building land with a rising sea. *Science* 349, 588–589. <https://doi.org/10.1126/science.aac8312>.
- Vuik, V., Jonkman, S.N., Borsje, B.W., Suzuki, T., 2016. Nature-based flood protection: the efficiency of vegetated foreshores for reducing wave loads on coastal dikes. *Coast. Eng.* 116, 42–56. <https://doi.org/10.1016/j.coastaleng.2016.06.001>.
- Vuik, V., van Vuren, S., Borsje, B.W., van Wesenbeeck, B.K., Jonkman, S.N., 2018. Assessing safety of nature-based flood defenses: dealing with extremes and uncertainties. *Coast. Eng.* 139, 47–64. <https://doi.org/10.1016/j.coastaleng.2018.05.002>.
- Yang, S.L., Shi, B.W., Bouma, T.J., Ysebaert, T., Luo, X.X., 2012. Wave attenuation at a salt marsh margin: a case study of an exposed coast on the Yangtze Estuary. *Estuaries Coasts* 35, 169–182. <https://doi.org/10.1007/s12237-011-9424-4>.
- Young, I.R., Zieger, S., Babanin, A.V., 2011. Global trends in wind speed and wave height. *Science* 332, 451–455. <https://doi.org/10.1126/science.1197219>.
- Ysebaert, T., Yang, S.-L., Zhang, L., He, Q., Bouma, T.J., Herman, P.M.J., 2011. Wave attenuation by two contrasting ecosystem engineering salt marsh macrophytes in the intertidal pioneer zone. *Wetlands* 31, 1043–1054. <https://doi.org/10.1007/s13157-011-0240-1>.